

Sm(Co,Fe,Cu,Zr)_z Magnets for High-Temperature Applications: Microstructural and Micromagnetic Analysis

T. Matthias, W. Scholz, *Member, IEEE*, J. Fidler, *Member, IEEE*, T. Schrefl, T. S. Rong, I. P. Jones, and I. R. Harris, *Senior Member, IEEE*

Abstract—The microstructure and the microchemistry of Sm(Co,Fe,Cu,Zr)_z permanent magnets determine the domain wall pinning behavior. This work combines nanoanalytical investigations of the precipitation structure with micromagnetic simulations. A cellular precipitation structure provides pinning centers. Measurements of the thickness of these precipitates by means of transmission electron microscopic image analysis and energy dispersive X-ray spectroscopy reveals that the average thickness is 15–18 nm, which is more than the calculated minimum value of 10 nm. Investigations of the elemental distribution across the precipitates show that the pinning behavior is repulsive.

Index Terms—Domain wall pinning, high-temperature magnets, microstructure, permanent magnets.

I. INTRODUCTION

Sm(Co,Fe,Cu,Zr)_z permanent magnets are the best choice for operating temperatures above 300 °C because of the high magnetocrystalline anisotropy and the high Curie temperature [1]–[3]. A complex production process, which involves sintering, homogenizing, isothermal aging and annealing results in the formation of a cellular precipitation structure which acts as pinning centers for magnetic domain walls [4]. The microstructure, which consists of the Sm₂(Co, Fe)₁₇ cell matrix phase, the Sm (Co, Cu)_{5–7} cell boundary phase and the Zr-rich lamella phase, develops mainly during the isothermal aging [5]. A numerical micromagnetic model based on the finite element (FE) method was developed in order to analyze the influence of variations in the microstructure as well as in the microchemistry on the coercive field. The micromagnetic model consists of 2 × 2 × 2 cells with a cell diameter of 125 nm (Fig. 1), which is consistent with measurements from transmission electron microscopy (TEM).

A change in the composition alters the microstructure as well as the microchemistry. Analysis of the high temperature magnetic properties of several series of Sm(Co_{bal}Fe_aCu_bZr_c)_z magnets showed that a high Sm content (after oxide correction) of 11.5–12.3, at.% ($z = 7, 7-7, 1$) results in the highest coercivity at 450 °C for a large range of compositions [6]. A mod-

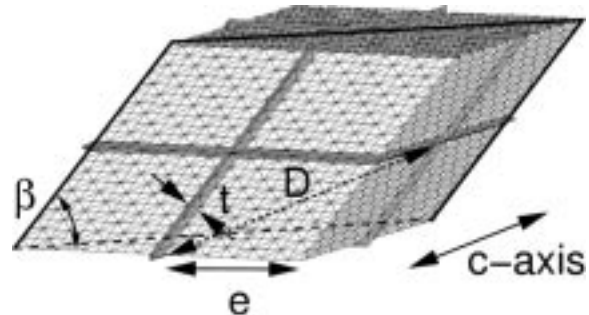


Fig. 1. Finite element model (FEM) of 2 × 2 × 2 cells with a cell diameter $D = 125$ nm and a variable cell boundary thickness t .

erately high Fe content of 10–15 at.% facilitates the sintering and increases the remanence [7]. Zr is necessary for the development of the lamella phase, which acts as a diffusion path during the heat treatment [8]. A high Zr content broadens the window of the possible Sm content [6], but at the cost of the remanence. Variations in the composition can directly be simulated through changes in the intrinsic magnetic properties of the involved phases.

As Cu segregates mainly to the Sm(Co, Cu)_{5–7} phase, the magnetocrystalline anisotropy of this phase can be tailored by the Cu content of the magnet [9]. As a result it is energetically favorable for a magnetic domain wall either to stay in the cell boundary phase (“attractive domain wall pinning,” if the domain wall energy is lower) or just inside the cells (“repulsive domain wall pinning,” if the domain wall energy in the cell boundary phase is higher than that in the cells).

Due to recent improvements in transmission electron microscopes, it is now possible to measure the elemental composition of the several phases on a scale of 1 nm.

II. EXPERIMENT

Samples with compositions of Sm(Co_{0.84}Cu_{0.13}Zr_{0.03})_{7.4} and Sm(Co_{0.74}Fe_{0.14}Cu_{0.08}Zr_{0.04})_{7.6}, hereafter referred to as samples A and B, were prepared using a typical powder metallurgy production route, including jetmilling, powder blending and compaction of oriented powder. The production process, using industrial equipment, and the magnetic properties have been described by Schobinger *et al.* [6]. Microstructural analysis was carried out using a JEOL JEM-200 CX and a FEI Tecnai F20 200 keV transmission electron microscope (TEM) equipped with a field emission gun.

Manuscript received February 15, 2002; revised April 28, 2002. This work was supported by the EC Project HITEMAG (GRD1-1999-11125).

T. Matthias, W. Scholz, J. Fidler, and T. Schrefl are with the Institut für Festkörperphysik, Vienna University of Technology, Vienna, Austria (e-mail: thorsten.matthias@tuwien.ac.at.).

T. S. Rong, I. P. Jones, and I. R. Harris are with the School of Metallurgy and Materials, University of Birmingham, Birmingham, U.K.

Digital Object Identifier 10.1109/TMAG.2002.803313.

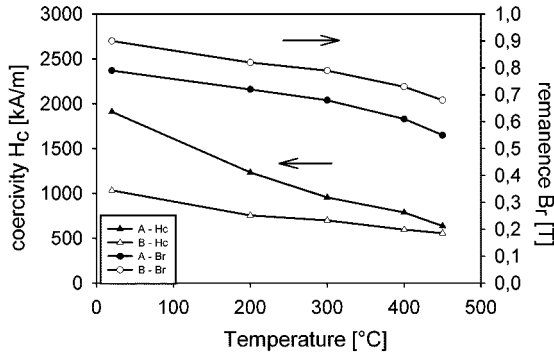


Fig. 2. Temperature dependence of coercivity and remanence of the magnets A and B.

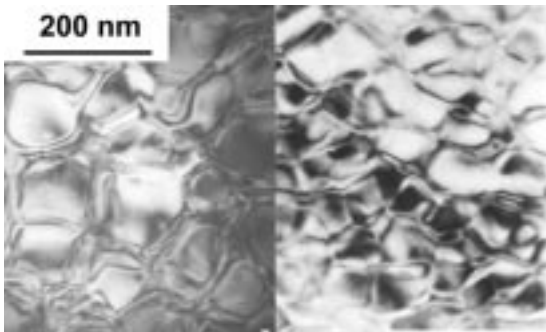


Fig. 3. Bright field images of samples A (left) and B (right).

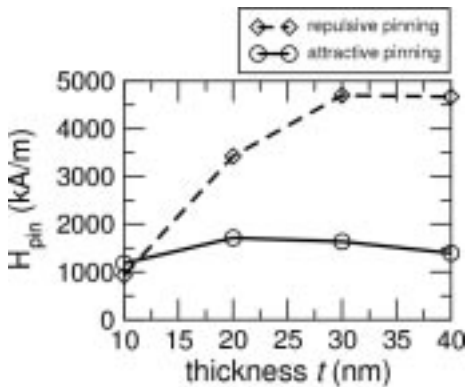


Fig. 4. Results of FE simulations: pinning field versus thickness of the cell boundary phase for different pinning mechanisms.

III. RESULTS

The composition of sample A with a high Cu content and without Fe results in a high coercivity H_c of 795 kA/m at 400 °C, but also in a low remanence B_r of 0,61 T at 400 °C. Sample B with a moderate Cu and Fe content has H_c of 597 kA/m and a B_r of 0,73 T at 400 °C. Fig. 2 shows the coercivity and remanence of A and B as a function of the temperature.

The microstructure of $\text{Sm}(\text{Co},\text{Fe},\text{Cu},\text{Zr})_z$ magnets can be tailored by the Sm content. A higher Sm content results in a higher volume fraction of the cell boundary phase, which, depending on the heat treatment, results either in thicker cell boundaries or in smaller cells. TEM analysis shows that, for an identical heat treatment, generally a smaller cellular structure is formed

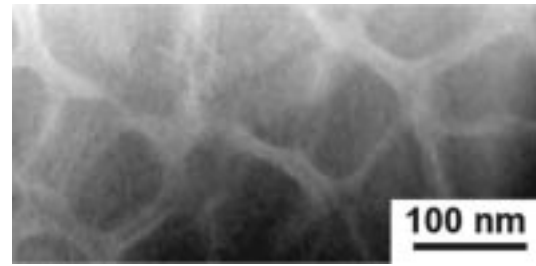


Fig. 5. High-angle annular dark field image of the precipitation structure of $\text{Sm}(\text{Co}_{0.74}\text{Fe}_{0.14}\text{Cu}_{0.08}\text{Zr}_{0.04})_{7.6}$.

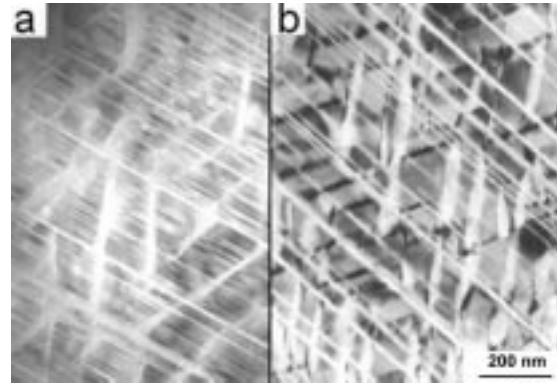


Fig. 6. Lamella phase of the samples (a) A and (b) B.

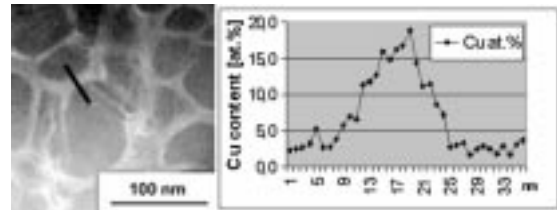


Fig. 7. Dark field image and corresponding X-ray line scan across a precipitate of sample A.

[10]. Fig. 3 shows that the cell structure of A is more homogeneous than that of B. The micromagnetic simulations show that a thicker cell boundary phase is favorable for a high coercivity (Fig. 4). This suggests that, if an optimized heat treatment were to result in larger cells with thicker cell boundaries, a higher coercivity could be achieved. A minimum thickness of 10 nm is necessary for a high coercive field of more than 1000 kA/m.

Fig. 5 shows a high-angle annular dark field (HAADF) image of the cellular precipitation structure of $\text{Sm}(\text{Co}_{0.74}\text{Fe}_{0.14}\text{Cu}_{0.08}\text{Zr}_{0.04})_{7.6}$. The contrast of the HAADF image is caused mainly by compositional differences and not by diffraction. The images show a projection of the real boundaries, which gives an upper limit for the cell boundary thickness of 18 nm. This is in good agreement with elemental X-ray line scans across the precipitates, which show an average thickness of the cell boundaries of about 15 nm (Fig. 7).

During the isothermal aging and annealing the Cu diffuses into the $\text{Sm}(\text{Co},\text{Cu})_{5-7}$ cell boundary phase. The lamella phase, which is important for the Cu distribution during the heat treatment, is very well developed in both samples (Fig. 6). Table I summarizes the Cu content within the cell matrix and the cell boundary phases of A and B. The differences in the Cu contents

TABLE I
AVERAGE Cu CONTENTS WITHIN THE CELL MATRIX (2:17)
AND THE CELL BOUNDARY (1:5) PHASE

sample	A (at.%)	B (at.%)
nominal Cu content	11,4	6,8
cell matrix phase	3,9 ± 0,8	2,9 ± 0,6
cell boundary phase	15,6 ± 1,2	11,9 ± 0,9

of the cell matrix phases show that the heat treatment is more appropriate for sample B than for sample A.

The Cu content also has a strong influence on the magnetocrystalline anisotropy: the higher the Cu content of a phase, the lower the magnetocrystalline anisotropy and the exchange interactions, because the phase becomes more and more paramagnetic. The coercive field of pinning controlled SmCo magnets is determined only by the difference in anisotropy between the cells and the cell boundary phase [9]. For very high Cu concentrations, very low magnetocrystalline anisotropy of the boundary phase may be assumed. Thus, the domain wall energy is lower in the boundary phase and attractive pinning is found. By its nature, the Sm(Co,Cu)₅-type boundary phase usually has a higher magnetocrystalline anisotropy than the cell matrix. The nanoanalytical measurements showed 15.6 and 11.9 at.% Cu in the cell boundaries of A and B, which reveals that these magnets show repulsive pinning.

IV. CONCLUSION

The analysis of the Cu and Zr contents shows that an optimized heat treatment is the key step toward high temperature permanent magnets. The remanence, a crucial parameter for technical applications, is decreased by Cu within the cell matrix phase as well as by the occurrence of Zr-Co phases, whereas the coercivity can be tailored by the Cu content in the Sm(Co, Cu)₅₋₇ phase. A high-energy density product requires an almost complete diffusion of Cu into the cell boundaries.

ACKNOWLEDGMENT

The authors wish to thank D. Schobinger and G. Martinek, Magnequench AG, Lupfig, Switzerland, for providing the magnets and O. Gutfleisch and D. Hinz, IFW Dresden, Dresden, Germany, for the magnetic measurements.

REFERENCES

- [1] K. J. Strnat, "Rare earth-cobalt permanent magnets," in *Ferromagnetic Materials*, E. P. Wohlfarth and K. H. J. Buschow, Eds, The Netherlands: North-Holland, 1988, vol. 4, pp. 131–209.
- [2] C. H. Chen, M. S. Walmer, M. H. Walmer, S. Liu, E. Kuhl, and G. Simon, "Sm₂(Co,Fe,Cu,Zr)₁₇ magnets for use at temperature > 400° C," *J. Appl. Phys.*, vol. 83, p. 6706, 1998.
- [3] G. C. Hadjipanayis, W. Tang, Y. Zhang, S. T. Chui, J. F. Liu, C. Chen, and H. Kronmueller, "High temperature 2:17 magnets: relationship of magnetic properties to microstructure and processing," *IEEE Trans. Magn.*, vol. 36, pp. 3382–3387, Sept. 2000.
- [4] J. Fidler, "Coercivity of precipitation hardened cobalt rare earth 17:2 permanent magnets," *J. MMM*, vol. 30, pp. 58–70, 1982.
- [5] J. Fidler, P. Skalicky, and F. Rothwarf, "High resolution Electron microscope study of Sm(Co,Fe,Cu,Zr)_{7,5} magnets," *IEEE Trans. Magn.*, vol. MAG-19, pp. 2041–2043, 1983.
- [6] D. Schobinger, O. Gutfleisch, D. Hinz, K.-H. Mueller, L. Schultz, and G. Martinek, "High temperature magnetic properties of 2:17 Sm-Co magnets," *J. MMM*, 2002, submitted for publication.
- [7] J. F. Liu, Y. Ding, and G. C. Hadjipanayis, "Effect of iron on the high temperature magnetic properties and microstructure of Sm(Co,Fe,Cu,Zr)_z permanent magnets," *J. Appl. Phys.*, vol. 85, pp. 1670–1674, 1999.
- [8] W. Tang, Y. Zhang, and G. C. Hadjipanayis, "Effect of Zr on the microstructure and magnetic properties of Sm(Co_{1-x}Fe_{0.1}Cu_{0.088}Zr_x)_{8,5} magnets," *J. Appl. Phys.*, vol. 87, pp. 399–403, 2000.
- [9] E. Lectard, C. H. Allibert, and R. Ballou, "Saturation magnetization and anisotropy in the Sm(Co_{1-x}Cu_x)₅ phases," *J. Appl. Phys.*, vol. 75, no. 10, pp. 6277–6279, 1994.
- [10] T. Matthias, G. Zehetner, J. Fidler, W. Scholz, T. Schrefl, D. Schobinger, and G. Martinek, "TEM-analysis of Sm(Co,Fe,Cu,Zr)_z magnets for high-temperature applications," *J. Magn. Magn. Mater.*, vol. 242–245, pp. 1353–1355, 2002.